Crack patterns induced by auto-stratification in drying sessile droplets of dairy proteins

C Le Floch-Fouéré, M Yu, F Boissel, Romain Jeantet, L Pauchard, L Lanotte

Colloids and Surfaces B: Biointerfaces 253 (2025) 114761

Contents lists available at ScienceDirect

Colloids and Surfaces B: Biointerfaces

journal homepage: www.elsevier.com/locate/colsurfb

Crack patterns induced by auto-stratification in drying sessile droplets of dairy proteins

C. Le Floch-Fouéré [a], M. Yu [a], F. Boissel [a], R. Jeantet [a], L. Pauchard [b], L. Lanotte [a,*]

[a] UMR STLO, INRAE, Institut Agro Rennes-Angers, Rennes 35000, France
[b] Laboratoire FAST, UMR 7608, CNRS – Université Paris-Saclay, Orsay 91405, France

ARTICLE INFO

Keywords:
Biocolloids
Evaporation
Protein stratification
Skin formation

ABSTRACT

Exploring the interfacial mechanisms involved in the evaporation of colloidal solutions is currently an open question with potential biomedical and industrial applications. In biological systems, unraveling evidence of self-arrangement is even more challenging due to the different size, structure and charge of their multi-components. In this work, we study the evaporation dynamics in mixes of dairy proteins, *i.e.*, whey proteins and casein micelles. Combining the observation of crack formation in drying droplets and the evaluation of the elastic response in films during the evaporation, we highlight interfacial stratification resulting in the external accumulation of whey proteins. We also relate such preferential segregation to the mechanical properties of the dry matrices, showing that whey protein overrepresentation confers a brittle behavior to the mixes. These experimental results enable the development of a first predictive model of the elastic modulus for biocolloid binary mixes, taking into account their deformability and different ratio in the samples. Unraveling the link between colloid self-arrangement and the evolution of skin properties during the evaporation is a first step towards controlling structure and use properties of the dry particles composing dairy powders.

1. Introduction

The dynamics of evaporation in colloidal systems have been intensively investigated in the last decades. The motivation for these studies often originated from the observation of everyday life events, from the evaporation of biological fluids (*e.g.*, sweat[1], teardrops[2]) to the traces left by widespread drinks on surfaces (*e.g.*, coffee[3], tea[4,5]). Over the years, several studies on droplets[6], films[7] and confined setups[8] revealed complex and often competitive drying-induced mechanisms, leading to different morphological scenarios, such as crack patterns[9,10], ordered deposits[11], strong interfacial deformations[12]. This rich variety of behaviors strongly depends on some external parameters, such as the characteristics of the substrate (*e.g.*, rugosity[13,14], charge[15], vibration[16]) and the environmental conditions (*e.g.*, temperature[17], relative humidity[18], pH[19,20]), but also on the intrinsic physicochemical properties of the colloids. In this regard, the impact of colloid size[21], shape[22] and deformability [23] on the development of the drying stages and the resulting deposits has been well characterized in the literature. Several works also aimed at identifying the possible link between drying-induced colloid arrangement and the mechanical properties of the samples[24-26]. These works highlighted a complex variety of behaviors that still need to be fully unraveled at the micron-scale.

The improved knowledge on the evaporation mechanisms in colloidal systems resulted in a gradual transition from fundamental physics studies to applicative research in a wide range of domains[27]. Indeed, interpreting the patterns left by biocolloidal samples is a potential tool for the conception of innovative biosensors or devices for fast diagnosis[10,28]. Tuning colloid self-assembly on a surface during the evaporation is nowadays a promising technique to design electronic devices[29] and filters with controlled pore size[30]. Shedding light on the dynamics of colloidal self-arrangement in free-falling droplets produced by spray drying[31] is key to optimize the process and consequently the quality of dry products. In the dairy industry, for example, controlling the functional and nutritional properties of milk powders is crucial to move towards more biomimetic high added value products, such as infant formulas[32] incorporating alive probiotic bacteria. To date, this represents an unsolved challenge, since the drying chambers used for dairy power production prevent the direct observation of droplet sol-gel transition and thus of the evaporation process.

For this reason, a series of works have been carried out in the last decade on the evaporation of single droplets of dairy solutions[33,34]

* Corresponding author.
E-mail address: luca.lanotte@inrae.fr (L. Lanotte).

https://doi.org/10.1016/j.colsurfb.2025.114761
Received 27 February 2025; Received in revised form 15 April 2025; Accepted 2 May 2025
Available online 7 May 2025

and, in particular, on simplified systems consisting of dairy proteins[35,36], *i.e.*, whey proteins and casein micelles. The main goal of these studies was to investigate the origin of the interfacial "skin" observed throughout the drying process[37], by analogy to other model colloidal systems reported in the literature[38,39]. The results highlighted the signature of the physicochemical properties of each protein on the formation/deformation of this skin and, consequently, on the morphological characteristics of the final dry grains. In agreement with previous theoretical and experimental studies on binary dispersions of model colloids[40-42], the investigation of drying droplets of dairy protein mixes led to the observation of a "small-on-top" behavior[43]. In short, the smaller colloids, *i.e.*, whey proteins in this specific case, gather on the external part of the skin due to diffusiophoretic phenomena and the osmotic pressure increasing during the evaporation process. It is plausible that this preferential protein segregation, whose occurrence depends inter alia on overall protein concentration and whey protein to casein micelle ratio, affects skin mechanical response and final shape of the grains. In Yu et al.[44], this hypothesis was indirectly explored characterizing droplet shape evolution, interfacial rheology and drying kinetics. However, a quantitative evaluation of the impact of protein interfacial self-assembly on skin mechanical properties is still lacking.

To fill this gap, in this paper we studied the macroscopic behavior of dispersions of whey protein and casein micelle mixes during the drying in two different configurations. We first provided a quantitative analysis of the formation of crack patterns in sessile droplets with the aim of revealing the response of the system to drying-induced internal stresses. Then, the mechanical response of dry films applying a localized external force was measured by indentations tests. Combining these two approaches, we corroborated the hypothesis of whey protein external accumulation in both configurations, and linked the dynamics of protein self-arrangement to the mechanical properties of the drying system. This enabled the formulation of a predictive model of the elastic modulus in a drying binary system consisting of colloids with different physico-chemical characteristics.

2. Materials and methods

2.1. Sample preparation

Whey protein isolate (WPI) and native phosphocaseinate (NPC) commercial powders, exhibiting 86 wt% and 82 wt% protein contents, respectively, were used to prepare suspensions with 10 wt% overall concentration. To this purpose, the powders were added to deionized water containing 0.02 wt% of sodium azide (NaN_3) as a bacteriostatic agent and stirred at room temperature (T = 20 °C) for 48 h to ensure full dissolution. Successively, WPI/NPC mixtures were obtained by mixing the WPI and NPC single protein suspensions at varying WPI relative percentages ($WPI\%_R$), defined as:

$$WPI\%_R = \frac{m_{WPI}}{m_{protein}} \quad (1)$$

Where m_{WPI} and $m_{protein}$ refer to the mass of WPI protein and total mass of proteins in the dispersions. In this study, $WPI\%_R$ was adjusted to 0, 20, 40, 50, 60, 80, 90, and 100 % to investigate the behavior of single proteins and the impact of protein ratio in the mixtures.

2.2. Microscopy

WPI/NPC droplets (V_0 = 0.5 μl) were deposited on glass coverslips previously cleaned by rinsing in ethanol and then water, and their evaporation was observed by an optical microscope (Olympus BX51) in bright field and phase contrast modalities. Image sequences were acquired by a QIClick camera and successively analyzed using a custom image analysis software (ImageJ). The experiments were performed under controlled environmental conditions, *i.e.*, temperature (T = 20 ± 1 °C) and relative humidity (RH = 40 %). Tests were repeated from 10 to 20 times for each $WPI\%_R$ value.

The morphology of dry WPI/NPC droplets, and in particular the transversal section corresponding to the crack opening was observed by scanning electron microscopy (JEOL JSM 7100 F) at an accelerating voltage of 10 KV, under high vacuum and working distance of 10 mm.

2.3. Micro-indentation tests

The mechanical properties of dried layers of WPI/NPC mixes were investigated by measuring their mechanical response to a load. A liquid layer was deposited in a container consisting of a circular silicon seal (diameter ~10 mm and height ~1 mm) adhering to a clean glass substrate. Water removal concentrated the solution until the formation of a solid layer of approximately constant thickness in the center of the container. Indentation tests were performed using a Micro-Hardness Tester - Anton Paar. A spherical indenter (Rockwell indenter of radius R_{ind} = 200 mm assumed to be perfectly rigid) was initially placed in contact with the surface of the film and, afterwards, directed into the dried layer with a controlled force, F (see the sketch in Fig. 7). To this purpose, the tip loading speed was kept at 100 $mN.min^{-1}$ until a maximum load was reached; the unloading process followed. Note that the maximum penetration depth reached by the indenter tip was always smaller than a tenth of the layer thickness. Measurements were carried out after the same drying time for each system, corresponding to the formation of a permanent crack network in the case of brittle systems.

3. Results

3.1. Colloid deposit and final morphology of droplets of WPI/NPC mixes

In this section, we aim at highlighting the link between the morphology of dry WPI/NPC droplets and the mechanisms of colloid deposit and arrangement occurring during drying. The outcomes for single protein solutions are first presented. Afterwards, a comparison with binary mixes is proposed to underline the different impact of WPI and NPC physico-chemical properties on the macroscopic characteristics of the dry droplets.

Whey proteins are globular macromolecules with an average size of 10–20 nm[45]. They mainly consist of β-lactoglobulins, often organized in dimers (molecular mass ≈ 36.6 kDa), and α-lactalbumins (molecular mass ≈ 14.2 kDa). A qualitative summary of the evaporation in WPI sessile droplets is presented in Fig. 1. Due to the border self-pinning, all the droplets exhibited a constant diameter with time for almost all the duration of the experiments. This favored the occurrence of outward capillary flows leading to the accumulation of proteins and the formation of an external "corona" (Fig. 1A). The gradual decrease of the droplet contact angle coupled with the simultaneous increase of centripetal internal stresses resulted in the phenomenon of stick-slip motion, consisting in the sudden reduction of the wet diameter and a successive new border pinning after a characteristic distance (Fig. 1B). At the end of the drying, when the water content in the WPI matrix is minimal, the considerable inward stresses were released by the formation of radial crack patterns (Fig. 1C). The typical opening phenomenon was initiated by the occurrence of so-called nucleation points in proximity of the triple line, where the colloid system is concentrated, and successively by the crack propagation towards the center of the droplets, as highlighted in Fig. 1C. Previous studies on the drying of globular proteins highlighted how the morphology and the complexity of these cracks are influenced by various and factors[10,46,47], such as protein molecular weight, concentration and pH.

Samples with NPC colloids, characterized by a sponge-like structure of 100–300 nm[48] and a molecular mass of ≈ 2.8 * 105 kDa, showed different deposits (Fig. 2). The early stage of the evaporation was characterized by the rapid formation of an external ring due to the fast evaporation at the so-called triple line (Fig. 2A). Most of all, very weak outward internal flows were noticed compared to whey proteins. This

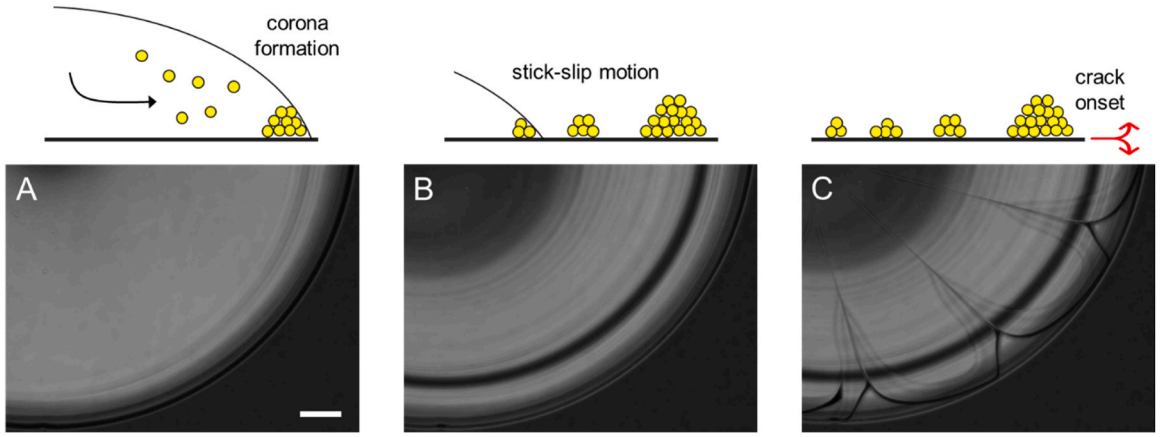

Fig. 1. Main stages of the drying process in WPI droplets summarized by images acquired in phase contrast mode coupled to schematic drawings: A) corona formation at droplet borders (t ≈ 4 min); B) stick-slip motion of the evaporation front (t ≈ 9 min); and C) radial cracks formation (t ≈ 16 min). Interference fringes reveal a delamination process.

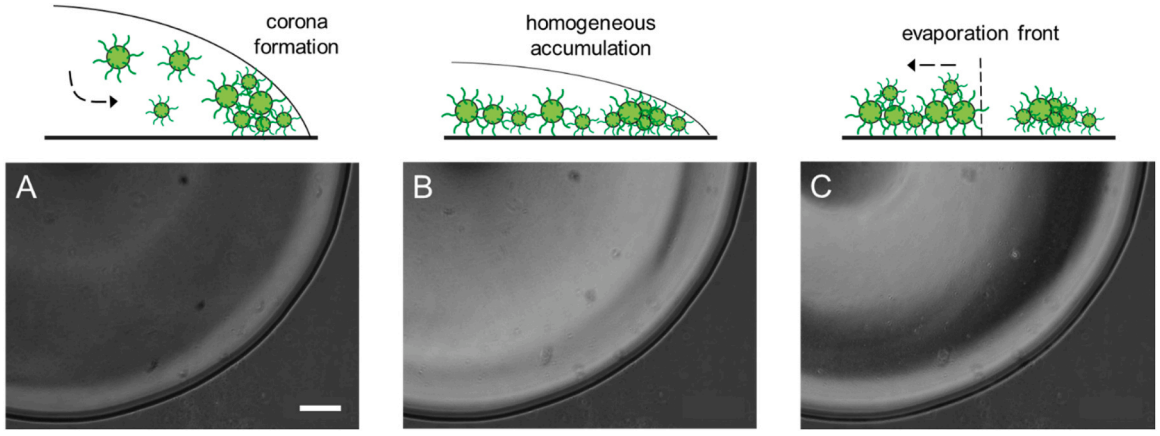

Fig. 2. Main stages of the drying process in WPI droplets summarized by images acquired in phase contrast mode coupled to schematic drawings: A) corona formation at droplet borders (t ≈ 3 min); B) protein homogeneous sedimentation on the substrate (t ≈ 7 min); and C) colloid inward migration (t ≈ 11 min).

can be probably attributed to the higher NPC volume fraction at the same mass concentration, as already underlined in previous works on the drying of milk proteins[44]. The absence of a significant colloid migration resulted in a homogeneous sedimentation on the substrate rather than in the real development of a corona (Fig. 2B). The uniform distribution of casein micelles was destabilized only when the drying process was advanced, and the retracting evaporation front transported the colloids inward (Fig. 2C).

As it concerns the morphology of droplets of WPI/NPC mixes at the end of the evaporation process, the images displayed in Fig. 3 highlight a gradual transition from NPC- to WPI-like shape with the increasing content of WPI in the mixture ($WPI\%_R$). Anyway, despite evident qualitative differences, in all the WPI/NPC droplets it was possible to recognize the specific signature of each protein, *i.e.*, radial cracks and concentric circles (especially for $WPI\%_R \geq 50$ %) in proximity of the borders for WPI and a deformed, wrinkled surface in the middle of the droplets for NPC. This suggests a colloidal segregation in the radial direction, with the whey proteins accumulating at droplet edges.

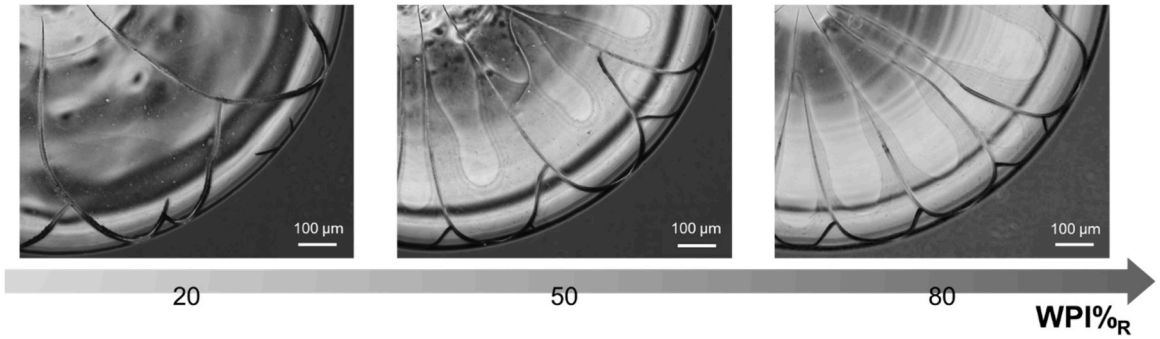

Fig. 3. Characteristic images of the shape of dry droplets of WPI/NPC mixes with $WPI\%_R$ ranging from 20 % to 80 %. The images were acquired by optical microscope in phase contrast mode.

3.2. Investigation of protein radial stratification in WPI/NPC droplets

The SEM observations mainly aimed at investigating the structure of the dry matter inside the open cracks and at highlighting possible evidence of colloid preferential arrangement and stratification. For example, the characteristic micrometric "canyons" corresponding to the radial cracks forming at the end of the evaporation in WPI solutions (Fig. 4, yellow square) were explored at the periphery (inset A) and in the center (inset B) of the droplets. In this case, no significant differences were detected between the two regions of interest and the section of the samples exhibited a smooth regular structure with the absence of relevant defects. This can be plausibly explained by the quite monodisperse size of whey protein molecules and their globular structure favoring the formation of a compact matrix.

When a minor amount of casein micelles was added to the mixture, *e.g.*, in the case of mixes with WPI%$_R$ = 80 % (Fig. 4, red square), the dry droplets exhibited an increased brittle character. In particular, the occurrence of orthoradial cracks was observed and the crack geometry became less regular moving from the periphery (inset C) to the center of the droplet (inset D). Mostly, this crack pattern modification also corresponded to a significant difference in terms of internal structure. Indeed, the transversal section of WPI%$_R$ = 80 % droplets in the vicinity of the borders consisted mainly of a smooth compact background surface, similar to what observed for WPI samples, net of scattered debris and alveoli. This could be seen as the clue of the presence of a second component in the dry matrix. On the other hand, the investigation of the central cracks revealed a highly rough and irregular surface, typical of NPC dry droplets (Figure S1). Similar results have been obtained in mixes with lower WPI amount (50 % $\leq$ WPI%$_R$ $\leq$ 80 %), thus corroborating the hypothesis of a preferential protein self-organization on the substrate, with the casein micelles accumulating at the center of the droplet.

In our experiments, the WPI/NPC droplets exhibited a low initial contact angle with the substrate at the triple line ($\alpha \approx 30°$) and border self-pinning. Under these experimental conditions, outward capillary flows predominate on Marangoni-like solute recirculation[28,49]. Consequently, we observed the gradual accumulation of the proteins on the substrate and especially at droplet borders, in analogy with the well-known coffee ring effect, rather than the formation of an interfacial skin. For this reason, the thoroughly investigated theory of the interfacial colloid stratification by size (*e.g.*, small-on-top)[38] does not apply in this case. The question of colloid separation in evaporating sessile droplets has been investigated in previous works[21,29,50] for possible applications in the development of diagnostic devices and the fabrication of biosensors. In these studies, which focused mainly on dilute binary suspensions, two main parameters have been identified as governing the phenomenon of particle sorting by size, *i.e.*, the colloid size ratio and the droplet surface tension[51,52]. Due to their higher diffusivity, the smaller colloids move faster towards the borders. Here, the droplet curvature acts as a steric limiting factor allowing only the particles with average smaller size to approach the triple line (except for a thin depletion zone). This leads to different colloid arrangement depending on the local colloid concentration near the periphery. In dilute regime, when the solvent is almost completely evaporated, liquid menisci envelop the particles already segregated by size. The surface tension overcomes the other forces acting on the colloids (*e.g.*, drag force, electrostatic and/or van der Waals interaction) and favors contact line depinning and further segregation of the two populations in separate rings[50]. In more crowded conditions, with the exception of a thin external corona of smaller colloids, an intermediate region is observable in which both types of particles are present[52]. The latter is the most probable scenario in the present study, especially in the light of the picture illustrated in the inset C of Fig. 4. In fact, due to the significantly different voluminosity of the two proteins, NPC volume fraction is always predominant compared to WPI one even at high WPI%$_R$, when whey proteins represent the major component in terms of mass concentration. This possibly leads to the insertion of NPC macromolecules in the highly ordered WPI matrix despite the favorable conditions for WPI segregation at droplet borders.

3.3. Impact of protein stratification on the drying stages

The following part of this study focuses on evaluating the impact of protein stratification on the mechanical behavior of WPI/NPC matrices in the droplets, from the onset of the cracks during the sol-gel transition to the achievement of the final morphology at the end of the process.

3.3.1. Sol-gel transition: crack occurrence

The development of the sol-gel transition, and in particular its final stage, was characterized in WPI/NPC droplets with different WPI%$_R$ by measuring the crack time, defined as the interval between the appearance of the first crack and the detection of the permanent final pattern. Concerning the onset of the cracks, the outcomes in Fig. 5 clearly show that they occurred gradually earlier with the increase of whey protein concentration in the samples. This is an indicator of the growing brittleness of the drying structure, as shown in a recent work on the

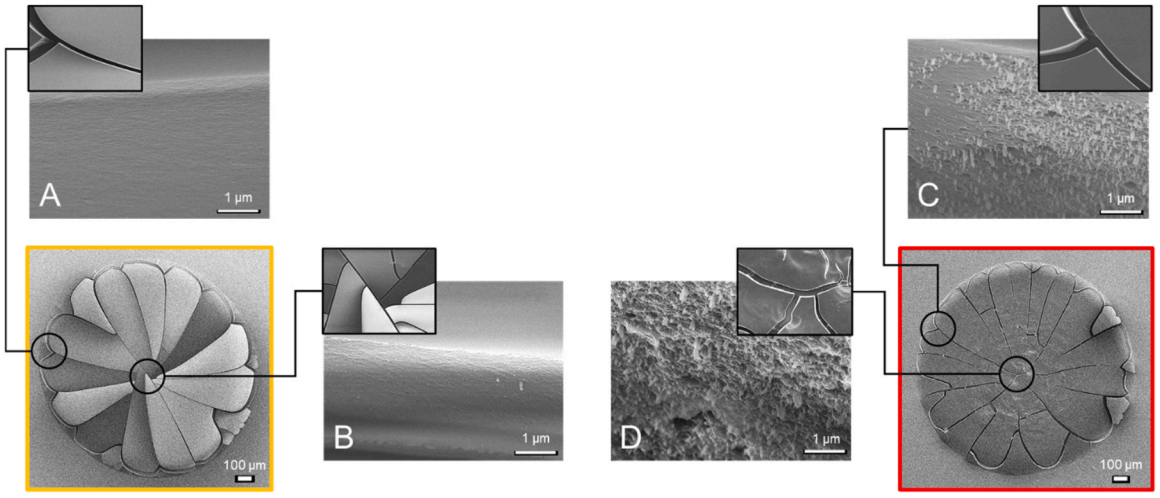

Fig. 4. Shape of droplets of WPI (yellow square) and WPI/NPC (red square) with WPI%$_R$ = 80 % observed by SEM microscope. In the insets, where the boxes depict high-magnification details of the black circles in the main pictures, the structure of the dry matter inside the cracks is shown for the border (A, C) and the middle (B, D) of both WPI and WPI/NPC samples, respectively.

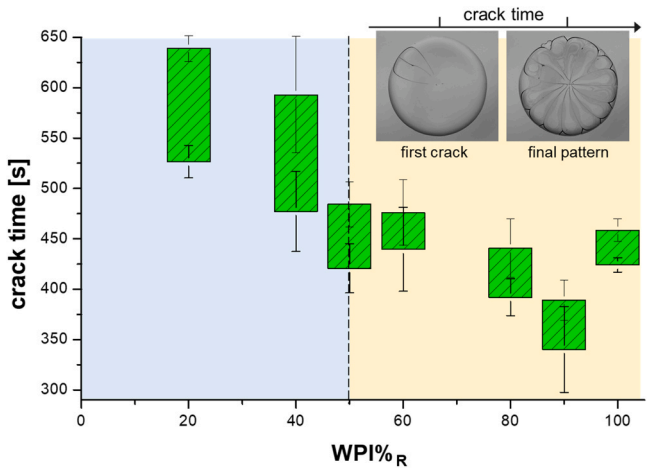

Fig. 5. Crack time, defined as the interval between the occurrence of the first crack and the achievement of the permanent crack pattern (see the inset), reported as a function of WPI/NPC mix composition ($WPI\%_R$). The light blue and light yellow areas highlight where the mechanisms of droplet sol-gel transition are influenced by NPC and WPI characteristics, respectively.

occurrence of crack patterns in drying nano-clay suspensions[53]. A possible interpretation lies in the higher compactness of NPC matrices compared to WPI ones. The deformability and the polydispersity of casein micelles would favor the gradual release of the increasing drying-induced stresses[48]. Interestingly, the only exception to this behavior was represented by the droplets with $WPI\%_R = 100$ %, which displayed a delayed crack time compared to other WPI-rich mixes. This unexpected trend reversal can be interpreted by the fact that a minimal presence of casein micelles (here corresponding to samples with $WPI\%_R = 80$ % and 90 %) is necessary to break the packed organization of the whey protein matrix (see Fig. 4, inset C), thus facilitating the fissure of the structure under mechanical solicitation.

As regards the crack time, our outcomes revealed the existence of two classes of mixes, characterized by similar duration, which are easily distinguishable in Fig. 5 by the sharp crack time reduction above a threshold value of $WPI\%_R \approx 50$ % (light yellow area). This specific ON-OFF behavior is possibly connected to the preferential segregation of WPI at droplet borders throughout the evaporation. Indeed, crack onset and propagation mainly occur in the vicinity of droplet edges, where whey proteins tend to accumulate. Therefore, drying-induced stress storage and release significantly depend on WPI self-arrangement close to the periphery when these colloids are sufficiently represented in the external corona, i.e., at higher $WPI\%_R$ values than 50 %.

A similar behavior was also observed in pendant WPI/NPC droplets in a recent article. In this work[44], the influence of WPI on the sol-gel dynamics was explained in the light of their outer stratification in the interfacial skin, which regulates the evaporation of the remaining water. In the present study, however, the evaporation front retracts radially inward without the formation of any skin and the region where WPI deposits are predominant is relatively thin, as highlighted in the inset C of Fig. 4. Consequently, further investigation is needed to fully elucidate how the overrepresentation of whey proteins at the borders can affect the mechanisms of crack formation.

3.3.2. Deduction of WPI/NPC matrix mechanical properties from crack pattern evaluation

The qualitative analysis of the morphology of dry WPI/NPC droplets illustrated in Fig. 1-3 pointed out that crack frequency and pattern characteristics are potentially a tool to estimate the material mechanical response to the internal stresses induced by water removal and colloid rearrangement. This approach has been borrowed from previous works on the directional drying of colloidal suspensions in confined geometries, *e.g.*, Hele-Shaw cells. From this point of view, Allain and Limat[9] have been the first to hypothesize that the wavelength, *i.e.*, the characteristic distance between cracks, depends on the competition between stress relaxation consequent to crack opening and stress increase due to solvent evaporation. Starting from these seminal findings, other works[8] aimed at characterizing the structure of dry colloidal matrices and their mechanical properties by the investigation of the regular crack patterns. In the specific case of our experiments far from being in confined conditions, the cracks were mostly radial rather than parallel. However, if considering the microscopic scale, the droplet curvature could be neglected in the proximity of the borders and, consequently, the approximation of parallelism would be still standing. For this reason, we measured here not only the number of cracks, but also the distance between consecutive cracks near the edges (λ) normalized by the height of the corona (δ) as a function of $WPI\%_R$ (see the inset of Fig. 6). The outcomes summarized in Fig. 6 show a qualitative agreement with what already illustrated for the occurrence of the cracks during the sol-gel transition (Fig. 5). Dry droplets exhibited an increasing number of cracks with higher whey protein concentration, with a trend reversal observed only for $WPI\%_R \geq 80$ %. This corroborates the hypothesis of brittle character conferred by WPI, further accentuated by irregularities due to NPC insertion in the packed structure for high values of $WPI\%_R$.

Evaluating the normalized crack distance mostly allowed to predict some mechanical properties of the dry structure and in particular its pore size (a). In the wake of previous works on the modeling of the crack opening in colloidal systems [54]Griffith, A. A. The Phenomena of Rupture and Flow in Solids, Philos. Trans. R. Soc. Lond. 221 163–198. Griffith, A. A. The Phenomena of Rupture and Flow in Solids. Philosophical Transactions of the Royal Society of London 221, 163–198.[54] we considered the energy balance referring to a representative volume (V) of thickness δ included between two consecutive cracks with characteristic distance λ. In this case, the elastic energy of the matrix must be equal to the energy necessary to create a new surface:

$$2\Gamma\lambda\delta = \frac{V}{2E}\langle\sigma\rangle^2 \tag{2}$$

where Γ is the surface energy of the newly created interfaces of typical area $\lambda\delta$ and here approximated to the water surface tension ($\approx 10^{-1}$ N.m^{-1}), E is the elastic modulus, and $<\sigma>$ is the average stress in the layer. This latter is defined as [55]:

$$\langle\sigma\rangle = \frac{\lambda}{\delta}P_{cap} \tag{3}$$

Here, P_{cap} is the capillary pressure, and it is calculated as [56]:

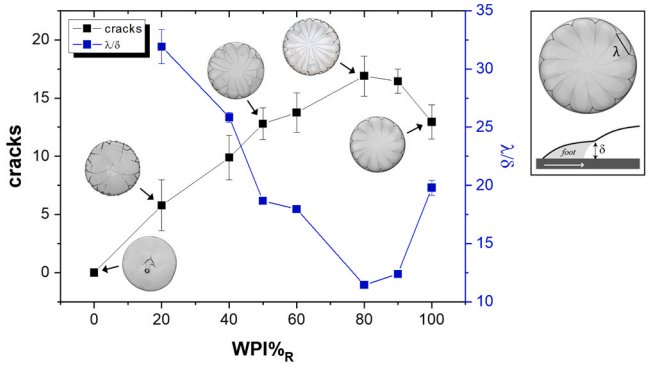

Fig. 6. Evolution of the number of cracks and the normalized distance between cracks (λ/δ) for different mix compositions ($WPI\%_R$). Examples of droplet typical shapes refer here to the corresponding $WPI\%_R$. The black and blue lines represent a guide for the eyes. The images in the inset illustrate how the parameter λ and δ have been measured.

$$P_{cap} = \frac{10\gamma}{a} \quad (4)$$

with γ being the surface tension of solvent, *i.e.*, water. Knowing that the volume V can be approximated to $\lambda^2\delta$, equation (2) can be restructured to obtain the matrix pore size:

$$a \approx \frac{\lambda\gamma}{\delta}\sqrt{\frac{\lambda}{10\Gamma E}} \approx \sqrt{\frac{\Gamma\lambda^3}{10E\delta^2}} \quad (5)$$

In equation (5), the only unknown parameter to estimate a is the value of the elastic modulus corresponding to the dry matrix. Due to the intrinsic difficulty to measure the mechanical response of WPI/NPC dry structures in the sessile droplet configuration adopted in this work, an alternative and simplified approach was necessary to estimate E. For this reason, micro-indentation tests were performed on films of WPI/NPC suspensions with same $WPI\%_R$ than single droplet experiments and drying under the same environmental conditions. In this setup, the drying-induced overrepresentation of the smaller colloids (*i.e.*, WPI) at the surface is highly predictable, in agreement with the "small-on-top" theory. Despite the different driving forces characterizing the colloid self-arrangement in sessile droplets and films, the same preferential segregation has been observed in both systems, thus making the matrix mechanical properties possibly comparable. On these bases, the loading/unloading curves resulting from layer's compressive axial stiffness are reported in Fig. 7A for different layers of WPI/NPC mixes. These curves revealed different elastic behaviors depending on the composition of the colloidal system. Assuming the material purely elastic within the limits of small deformations, the elastic response is well fitted using the Hertz contact [57]:

$$F = \frac{4\sqrt{R_{ind}}}{3(1-\nu^2)}p^{3/2} \quad (6)$$

Where p is the penetration depth of the indenter tip and ν is the Poisson's ratio of the layer, assumed to be 0.3 as classically adopted for colloids[58]. The resulting elastic modulus, E, is plotted as a function of the $WPI\%_R$ in Fig. 7B. Within the same range of loading, the penetration depth was almost 5 times lower in layers of casein micelles compared to samples with $WPI\%_R \geq 50$ %. Moreover, the latter exhibited a significant hysteresis. This suggests that, once the packed WPI matrix is broken, it does not show any elastic response. On the contrary, NPC films tended to return to the initial configuration once the force F was no longer acting on the surface.

The quantification of the mechanical response of WPI/NPC dry matrices resulted in the deduction of their average pore size for different sample compositions using equation (5), as reported in Table 1. Similar to what observed on crack pattern formation, the trend regarding a is characterized by a minimum for $WPI\%_R = 80$ %. This strongly corroborates the hypothesis of a particular interfacial protein self-arrangement at this specific WPI relative percentage, leading to enhanced brittle characteristics.

As a last step, a predictive model of the elastic modulus of WPI/NPC layers as a function of $WPI\%_R$ and protein mechanical properties is also proposed in Fig. 7B. In this regard, some approximations have been made. First, we considered the dried layers of proteins as an assembly of spheres with radius equal to 100 nm for NPC (r_{NPC}) and 4 nm for WPI samples (r_{WPI}), thus comparable to the average size of the native proteins. The same Poisson ratio was taken into account for both proteins ($\nu = 0.3$). We also assumed that the surface energy (Γ) bonding the idealized spheres together is the same whatever the type and number of spheres in contact and its value is equal to 10^{-1} N.m^{-1} (water surface tension). On the bases of previous works in the literature, the elastic modulus of the packing of one type of spheres (WPI or NPC) was taken proportional to [59]:

$$E_i \propto \left(\Gamma e_i^2 / r_i\right)^{1/3} \quad (7)$$

Where the prefactor depends on the packing and the number of contacts between the spheres (close to 10)[60]. E_{NPC} and E_{WPI} are the values of the elastic moduli of dried NPC ($WPI\%_R = 0$ %) and WPI ($WPI\%_R = 100$ %).

For a binary mixture of particles exhibiting different stiffnesses and sizes, the elastic response was represented by a harmonic average[61], where the elastic modulus and the size corresponding to single proteins were indicated by e_i and r_i, respectively. This results in the elastic modulus, e_{mix}, and the effective size, r_{mix}, of the combination of spheres, equal to

Table 1
Estimation of the pore size (a) of WPI/NPC dry matrices with different composition ($WPI\%_R$) obtained by the evaporation of films of protein mixes.

$WPI\%_R$	Pore size, a (nm)
20	10.30
50	8.34
80	4.29
100	8.55

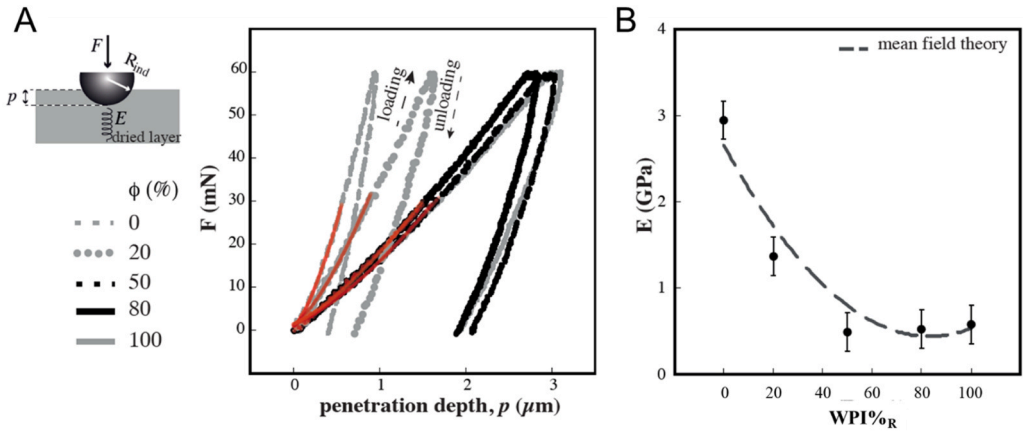

Fig. 7. Evaluation of the mechanical behavior of WPI/NPC dry films with different $WPI\%_R$ using micro-indentation. The side view sketch on the left illustrates the penetration of a spherical indenter into the dry material. (a) The load, F, applied to materials is plotted as a function of the penetration depth, p, of the indenter tip. The red lines are the theoretical predictions within the limits of small axial compression in accordance with the Hertz contact law. (b) Elastic modulus, E, deduced from the Hertz theory as a function of $WPI\%_R$ in the dried layers. The dashed grey line is the macroscopic response of a dense packing of spherical particles in accordance with equation (6).

$$e_{mix}{}^{-1} = (e_{NPC}{}^{-1} + e_{WPI}{}^{-1})^{-1} \quad (8)$$

and

$$\mathrm{r_{mix}}^{-1} = (\mathrm{r_{NPC}}^{-1} + \mathrm{r_{WPI}}^{-1})^{-1} \quad (9)$$

respectively[62]. The elastic modulus, E_{mix}, of the binary mixture is obtained by incorporating e_{mix} and $\mathrm{r_{mix}}$ into the equation (7).

The macroscopic response of a dense packing of spherical particles was investigated by Russel et al.[63]. In this mean-field approach, the affine deformation of each pair of contacting particles and the average over all orientations of contact surface is assumed:

$$\overline{E} \propto (1 - \mathrm{WPI\%_R})^2 E_{NPC} + 4\mathrm{WPI\%_R}(1 - \mathrm{WPI\%_R})E_{mix} + \mathrm{WPI\%_R}{}^2 E_{WPI} \quad (10)$$

where E_{NPC} and E_{WPI} are the elastic moduli of a dried layer of single NPC ($\mathrm{WPI\%_R} = 0$ %) and WPI ($\mathrm{WPI\%_R} = 100$ %) proteins, respectively. Equation (10) was used to obtain a predictive curve of E as a function of WPI relative percentage (dashed line in Fig. 7B), showing a good agreement with the trend of the experimental data. The elastic moduli of the spheres modelling the NPC and WPI are adjustable parameters. Here, the best fit is obtained for $E_{WPI} = 10^9$ Pa, $\mathrm{r_{WPI}} = 8$ nm and $E_{NPC} = 3.10^9$ Pa, $\mathrm{r_{NPC}} = 100$ nm. Although improvable and based on strong approximations, this simple model represents a first step towards the prediction and the control of dairy powder functional properties.

4. Conclusions

In this work, we provide a direct observation of protein self-sorting during the evaporation of sessile droplets of mixes of whey proteins and casein micelles. The impact of WPI external segregation on the mechanical properties of the dry matrices was first evaluated by the investigation of the sol-gel transition and, in particular, of crack pattern formation in WPI/NPC droplets. In parallel, we measured the mechanical response of dry WPI/NPC layers resulting from the evaporation of films with same composition ($\mathrm{WPI\%_R}$) by indentation tests, obtaining consistent agreement with the case of sessile droplets. The results obtained are in agreement with previous studies on model colloids, showing the preferential accumulation of WPI at the borders due to their smaller size and droplet curvature (*i.e.*, surface tension). The integration of the experimental results also favored the elaboration of a first predictive model of the elastic modulus (E) of the dry WPI/NPC structures as a function of $\mathrm{WPI\%_R}$. Interestingly, both crack pattern evaluation and indentation measures highlighted a singular macroscopic behavior for $\mathrm{WPI\%_R} \approx 80$ %, possibly related to a specific protein self-arrangement at the interface that will require further and deepened investigation. A logical development of this study will be taking into account the effect of the evaporation rate on the mechanical properties of WPI/NPC matrices and, thus, further validating our predictive approach.

CRediT authorship contribution statement

C. Le Floch-Fouéré: Writing – review & editing, Validation, Supervision, Methodology, Conceptualization. **M. Yu:** Investigation, Formal analysis. **F. Boissel:** Investigation. **R. Jeantet:** Writing – review & editing, Validation, Supervision, Conceptualization. **Luca Lanotte:** Writing – review & editing, Writing – original draft, Visualization, Validation, Supervision, Methodology, Investigation, Formal analysis, Data curation, Conceptualization. **L. Pauchard:** Writing – original draft, Validation, Methodology, Investigation, Conceptualization.

Declaration of Competing Interest

The authors declare that they have no known competing financial interests or personal relationships that could have appeared to influence the work reported in this paper.

Appendix A. Supporting information

Supplementary data associated with this article can be found in the online version at doi:10.1016/j.colsurfb.2025.114761.

Data availability

Data will be made available on request.

References

[1] M. Gonçalves, et al., Droplet evaporation on porous fabric materials, Sci. Rep. 12 (2022) 1087.
[2] L.C. Madden, A. Tomlinson, P.A. Simmons, Effect of Humidity Variations in a Controlled Environment Chamber on Tear Evaporation After Dry Eye Therapy, Eye Contact Lens: Sci. Clin. Pract. 39 (2013) 169–174.
[3] J.Y. Kim, B.M. Weon, Evaporation of strong coffee drops, Appl. Phys. Lett. 113 (2018) 183704.
[4] Y. Tanizawa, T. Abe, K. Yamada, Black tea stain formed on the surface of teacups and pots. Part 1 – Study on the chemical composition and structure, Food Chem. 103 (2007) 1–7.
[5] K. Yamada, T. Abe, Y. Tanizawa, Black tea stain formed on the surface of teacups and pots. Part 2 – Study of the structure change caused by aging and calcium addition, Food Chem. 103 (2007) 8–14.
[6] K. Sefiane, Patterns from drying drops, Adv. Colloid Interface Sci. 206 (2014) 372–381.
[7] A.F. Routh, Drying of thin colloidal films, Rep. Prog. Phys. 76 (2013) 046603.
[8] E.R. Dufresne, et al., Dynamics of Fracture in Drying Suspensions, Langmuir 22 (2006) 7144–7147.
[9] C. Allain, L. Limat, Regular Patterns of Cracks Formed by Directional Drying of a Collodial Suspension, Phys. Rev. Lett. 74 (1995) 2981–2984.
[10] T.A. Yakhno, et al., Drying drops of biological liquids: dynamics of the optical and mechanical properties. Application in rapid medical diagnostics, Proc. SPIE 5692 (2015) 188–198.
[11] N. Denkov, et al., Mechanism of formation of two-dimensional crystals from latex particles on substrates, Langmuir 8 (1992) 3183–3190.
[12] F. Boulogne, F. Giorgiutti-Dauphiné, L. Pauchard, The buckling and invagination process during consolidation of colloidal droplets, Soft Matter 9 (2013) 750–757.
[13] T. Pham, S. Kumar, Drying of Droplets of Colloidal Suspensions on Rough Substrates, Langmuir 33 (2017) 10061–10076.
[14] T.A.H. Nguyen, M.A. Hampton, A.V. Nguyen, Evaporation of Nanoparticle Droplets on Smooth Hydrophobic Surfaces: The Inner Coffee Ring Deposits, J. Phys. Chem. C. 117 (2013) 4707–4716.
[15] F. Fan, K.J. Stebe, Assembly of Colloidal Particles by Evaporation on Surfaces with Patterned Hydrophobicity, Langmuir 20 (2004) 3062–3067.
[16] T. Muangnapoh, A.L. Weldon, J.F. Gilchrist, Enhanced colloidal monolayer assembly via vibration-assisted convective deposition, Appl. Phys. Lett. 103 (2013) 181603.
[17] N.D. Patil, P.G. Bange, R. Bhardwaj, A. Sharma, Effects of Substrate Heating and Wettability on Evaporation Dynamics and Deposition Patterns for a Sessile Water Droplet Containing Colloidal Particles, Langmuir 32 (2016) 11958–11972.
[18] F. Girard, M. Antoni, S. Faure, A. Steinchen, Influence of heating temperature and relative humidity in the evaporation of pinned droplets, Colloids Surf. A: Physicochem. Eng. Asp. 323 (2008) 36–49.
[19] R. Bhardwaj, X. Fang, P. Somasundaran, D. Attinger, Self-Assembly of Colloidal Particles from Evaporating Droplets: Role of DLVO Interactions and Proposition of a Phase Diagram, Langmuir 26 (2010) 7833–7842.
[20] L. Pauchard, F. Parisse, C. Allain, Influence of salt content on crack patterns formed through colloidal suspension desiccation, Phys. Rev. E 59 (1999) 3737–3740.
[21] S. Chatterjee, J.S. Murallidharan, R. Bhardwaj, Size-Dependent Dried Colloidal Deposit and Particle Sorting via Saturated Alcohol Vapor-Mediated Sessile Droplet Spreading, Langmuir 38 (2022) 6128–6147.
[22] P.J. Yunker, et al., Effects of Particle Shape on Growth Dynamics at Edges of Evaporating Drops of Colloidal Suspensions, Phys. Rev. Lett. 110 (2013) 035501.
[23] M. Jose, M. Mayarani, M.G. Basavaraj, D.K. Satapathy, Evaporative self-assembly of the binary mixture of soft colloids, Phys. Chem. Chem. Phys. 23 (2021) 7115–7124.
[24] L. Goehring, W.J. Clegg, A.F. Routh, Plasticity and Fracture in Drying Colloidal Films, Phys. Rev. Lett. 110 (2013) 024301.
[25] A. Hari Govindha, P. Katre, S. Balusamy, S. Banerjee, K.C. Sahu, Counter-intuitive evaporation in nanofluids droplets due to stick-slip nature, Langmuir 38 (2022) 15361–15371.
[26] V. Lazarus, L. Pauchard, From craquelures to spiral crack patterns: influence of layer thickness on the crack patterns induced by desiccation, Soft Matter 7 (2011) 2552.
[27] P. Bacchin, et al., Drying colloidal systems: Laboratory models for a wide range of applications, Eur. Phys. J. E 41 (2018) 94.
[28] A. Pal, A. Gope, A. Sengupta, Drying of bio-colloidal sessile droplets: Advances, applications, and perspectives, Adv. Colloid Interface Sci. 314 (2023) 102870.
[29] W. Han, M. Byun, Z. Lin, Assembling and positioning latex nanoparticles via controlled evaporative self-assembly, J. Mater. Chem. 21 (2011) 16968.
[30] H. Zargartalebi, S.H. Hejazi, A. Sanati-Nezhad, Self-assembly of highly ordered micro- and nanoparticle deposits, Nat. Commun. 13 (2022) 3085.

[31] E. Lintingre, F. Lequeux, L. Talini, N. Tsapis, Control of particle morphology in the spray drying of colloidal suspensions, Soft Matter 12 (2016) 7435–7444.
[32] A. Deglaire, et al., Towards more biomimetic and sustainable infant formula: challenges and future opportunities, Trends Food Sci. Technol. 137 (2023) 109–123.
[33] M.A.I. Schutyser, J. Perdana, R.M. Boom, Single droplet drying for optimal spray drying of enzymes and probiotics, Trends Food Sci. Technol. 27 (2012) 73–82.
[34] N. Fu, M.W. Woo, X.D. Chen, Colloidal transport phenomena of milk components during convective droplet drying, Colloids Surf. B: Biointerfaces 87 (2011) 255–266.
[35] C. Sadek, et al., Shape, Shell, and Vacuole Formation during the Drying of a Single Concentrated Whey Protein Droplet, Langmuir 29 (2013) 15606–15613.
[36] C. Sadek, et al., Buckling and collapse during drying of a single aqueous dispersion of casein micelle droplet, Food Hydrocoll. 52 (2016) 161–166.
[37] C. Sadek, et al., Mechanical properties of milk protein skin layers after drying: Understanding the mechanisms of particle formation from whey protein isolate and native phosphocaseinate, Food Hydrocoll. 48 (2015) 8–16.
[38] W. Liu, J. Midya, M. Kappl, H.-J. Butt, A. Nikoubashman, Segregation in Drying Binary Colloidal Droplets, ACS Nano 13 (2019) 4972–4979.
[39] M. Nassar, A. Gromer, F. Thalmann, P. Hébraud, Y. Holl, Velocity of lateral drying fronts in film formation by drying of colloidal dispersions. A 2D simulation, J. Colloid Interface Sci. 511 (2018) 424–433.
[40] J. Zhou, Y. Jiang, M. Doi, Cross-interaction drives stratification in drying film of binary colloidal mixtures, Phys. Rev. Lett. 118 (2017) 108002.
[41] R.P. Sear, P.B. Warren, Diffusiophoresis in nonadsorbing polymer solutions: The Asakura-Oosawa model and stratification in drying films, Phys. Rev. E 96 (2017) 062602.
[42] M. Schulz, J.L. Keddie, A critical and quantitative review of the stratification of particles during the drying of colloidal films, Soft Matter 14 (2018) 6181–6197.
[43] L. Lanotte, F. Boissel, P. Schuck, R. Jeantet, C. Le Floch-Fouéré, Drying-induced mechanisms of skin formation in mixtures of high protein dairy powders, Colloids Surf. A: Physicochem. Eng. Asp. 553 (2018) 20–27.
[44] M. Yu, et al., Skin layer stratification in drying droplets of dairy colloids, Colloids Surf. A: Physicochem. Eng. Asp. 620 (2021) 126560.
[45] Y.F. Yano, Kinetics of protein unfolding at interfaces, J. Phys.: Condens. Matter 24 (2012) 503101.
[46] A. Sett, M. Ayushman, S. Dasgupta, S. Dasgupta, Analysis of the Distinct Pattern Formation of Globular Proteins in the Presence of Micro- and Nanoparticles, J. Phys. Chem. B 122 (2018) 8972–8984.
[47] A. Pal, A. Gope, A.S. Athair, G.S. Iannacchione, A comparative study of the drying evolution and dried morphology of two globular proteins in de-ionized water solutions, RSC Adv. 10 (2020) 16906–16916.
[48] A. Bouchoux, G. Gésan-Guiziou, J. Pérez, B. Cabane, How to Squeeze a Sponge: Casein Micelles under Osmotic Stress, a SAXS Study, Biophys. J. 99 (2010) 3754–3762.
[49] R.D. Deegan, et al., Capillary flow as the cause of ring stains from dried liquid drops, Nature 389 (1997) 827–829.
[50] N.D. Patil, R. Bhardwaj, A. Sharma, Self-sorting of Bi-dispersed Colloidal Particles near Contact Line of an Evaporating Sessile Droplet, Langmuir 34 (2018) 12058–12070.
[51] C. Monteux, F. Lequeux, Packing and Sorting Colloids at the Contact Line of a Drying Drop, Langmuir 27 (2011) 2917–2922.
[52] P.A. Zolotarev, K.S. Kolegov, Monte Carlo simulation of particle size separation in evaporating bi-dispersed colloidal droplets on hydrophilic substrates, Phys. Fluids 34 (2022) 017107.
[53] V.R.S. Parmar, R. Bandyopadhyay, Manipulating crack formation in air-dried clay suspensions with tunable elasticity, Phys. Fluids 36 (2024) 113114.
[54] Griffith, A. A. The Phenomena of Rupture and Flow in Solids, Philos. Trans. R. Soc. Lond. 221 (1921) 163–198.
[55] X. Ma, J. Lowensohn, J.C. Burton, Universal scaling of polygonal desiccation crack patterns, Phys. Rev. E 99 (2019) 012802.
[56] W.P. Lee, A.F. Routh, Why Do Drying Films Crack? Langmuir 20 (2004) 9885–9888.
[57] A.C. Fischer-Cripps, Contact Mechanics. *Nanoindentation. Mechanical Engineering Series.*, Springer, New York, NY, 2024 (in).
[58] E. Di Giuseppe, A. Davaille, E. Mittelstaedt, M. François, Rheological and mechanical properties of silica colloids: from Newtonian liquid to brittle behaviour, Rheol. Acta 51 (2012) 451–465.
[59] K. Kendall, N.McN Alford, J.D. Birchall, Elasticity of particle assemblies as a measure of the surface energy of solids, Proc. R. Soc. Lond. A 412 (1987) 269–283.
[60] K. Kendall, N. McN.Alford, J.D. Birchall, A new method for measuring the surface energy of solids, Nature 325 (1987) 794–796.
[61] L. Pauchard, B. Abou, K. Sekimoto, Influence of Mechanical Properties of Nanoparticles on Macrocrack Formation, Langmuir 25 (2009) 6672–6677.
[62] T. Lachhab, C. Weill, Compression of a soft sphere packing, Eur. Phys. J. B 9 (1999) 59–69.
[63] W.B. Russel, N. Wu, W. Man, Generalized Hertzian Model for the Deformation and Cracking of Colloidal Packings Saturated with Liquid, Langmuir 24 (2008) 1721–1730.